DOI: 10.1089/ees.2007.0076

Properties of Membranes Containing Semi-dispersed Carbon Nanotubes

L. Brunet,[1] D.Y. Lyon,[1] K. Zodrow,[1] J.-C. Rouch,[2] B. Caussat,[3] P. Serp,[4] J.-C. Remigy,[2] M.R. Wiesner,[5*] and P.J.J. Alvarez[1]

[1]Department of Civil and Environmental Engineering
Rice University
Houston TX 77005

[2]Laboratoire de Génie Chimique UMR-CNRS 5503
Université Paul Sabatier
31062 Toulouse Cedex, France

[3]Laboratoire de Génie Chimique UMR-CNRS 5503
Ecole Nationale Supérieure d'Ingénieurs en Arts Chimiques et Technologiques
31106 Toulouse Cedex 1, France

[4]Laboratoire de Chimie de Coordination UPR 8421-CNRS
Ecole Nationale Supérieure en Arts Chimiques et Technologiques
Toulouse Cedex, France

[5]Department of Civil and Environmental Engineering
Duke University
Durham, NC 27708-0287

ABSTRACT

Carbon nanotubes exhibit superior mechanical and electrical properties that make them attractive for developing new composite materials. In this research, we examined the properties of ultrafiltration membranes made from carbon nanotube/polymer composites. Multiwalled carbon nanotubes (MWCNT, 4% w/w) were incorporated into polysulfone ultrafiltration membranes, prepared according to the wet phase inversion method. The dispersion of the nanotubes and the morphology of the membranes were observed by scanning electron microscopy. The membranes were characterized for surface roughness, contact angle, permeability, and mechanical properties. A partial deaggregation of the nanotubes leads to individual nanotubes within the polymer as well as bundles nested in the pores. After addition of MWCNTs, the assymetric structure of the membrane, the permeability, and the hydrophobicity were not disturbed, but the roughness increased. Contrary to expectations, the tensile strength of the composite membrane was not improved while the elongation to failure decreased because of a lack of dispersion of the nanotubes. Growth of bacteria on the membranes was tested using two different methods, neither of which indicated an antibacterial effect due to the presence of nanotubes.

Key words: carbon nanotubes; polymeric membrane; water treatment; reinforcement; biofouling

*Corresponding author: Department of Civil and Environmental Engineering, Duke University, Durham, NC 27708-0287. *E-mail:* wiesner@duke.edu

INTRODUCTION

The potential of the mechanical and electrical properties of carbon nanotubes (CNTs), as well as their biological applications, has created considerable interest in the scientific and technical communities since their discovery by Iijima in 1991 (Iijima, 1991). Numerous applications of these materials have been proposed, leading to a virtual race to produce quantities of high-quality multiwalled (MW) and single-walled carbon nanotubes (SWCNTs) at the industrial scale. In this communication, we explore the use of CNTs in the development of advanced composite membranes for applications in water treatment. Recent studies have considered the properties and advantages of polymer CNT composites (Barrera, 2000; Kearns and Shanbaugh, 2002; Safadi *et al.*, 2002; Coleman *et al.*, 2006). Many practical challenges remain before the potential of CNT composites can be fully realized. Notably, uniform dispersion of distinct nanotubes in the polymer matrix as well as a good interfacial bonding are required. These challenges would seem to be even greater in membrane fabrication, as issues such as the porosity of the medium or the presence of additives must also be addressed.

There are several potential advantages of the use of CNT composites for water treatment. First, the possible toxicity of some fullerenes towards bacteria might be exploited when dispersed in membranes. Currently, most of the toxicological evaluations conducted on cultured cells or *in vivo* support the toxicity of CNTs (Ding *et al.*, 2005; Lam *et al*., 2006) even if the response depended on the degree of sidewall functionalization (Sayes *et al.*, 2006). In one study, MWCNTs caused cell death and apoptosis with corresponding changes in the protein expression of human skin fibroblasts, although this study did not conclusively define the mechanism of cell death (Ding *et al.*, 2005). Another study with *Escherichia coli* demonstrated how MWCNTs are able to form temporary "nanochannels" in the cell membrane, leading to a decrease in cell viability (Rojas-Chapana *et al*., 2005). If such toxic effects were confirmed, CNTs immobilized within the membrane skin might serve as a basis for inhibiting bacterial growth and therefore reducing biofouling. Narayan *et al.* (2005) successfully manufactured carbon nanotube composite films with antibacterial properties in the hopes of reducing biofilm formation.

Another potential advantage of CNT incorporation in membranes is facile alteration of the membrane properties by manipulating the properties of the CNT. Nanotubes can be functionalized to create materials of variable hydrophilicity that might be used to adjust membrane surface chemistry (Choi *et al.*, 2006). Chemical modification of membrane surfaces through the introduction of nanomaterials can alter the affinity of the membrane for organic solutes and reduce fouling.

Perhaps the greatest advantage is that SWCNTs and high-quality MWCNTs prepared by arc-discharge exhibit a high surface area and unique characteristics: their Young's moduli can reach values greater than 1 TPa and the tensile strength can be as high as 50 GPa (Coleman *et al.*, 2006). One premise of the current effort is that these properties might be exploited to create membrane materials of very high strength. While MWCNTs produced by chemical vapor deposition (CVD) generally have more defects and therefore display poorer mechanical properties (Coleman *et al.*, 2006), they nonetheless share these properties and are the most widely available CNTs.

Membrane breakage and decreased performance over time due to fouling, especially biofouling, are two major problems that induce high maintenance costs in drinking water treatment applications. Our broad objective is to develop high-performance membranes that are robust enough to endure the high pressures generally involved in ultrafiltration and nanofiltration. In this work, we consider the effect of MWCNTs, at a loading of 4% w/w using polyvinylpyrrolidone (PVP) as an additive, on the morphology of polysulfone (PSF) ultrafiltration membranes and on their mechanical, surface, hydraulic, and antibiofouling properties.

EXPERIMENTAL SECTION

Membrane fabrication

Materials. Polysulfone beads (PSF -UDEL® P3500) were provided by Solvay (Brussels, Belgium). *N*-Methyl-2-pyrrolidone (NMP) used as PSF solvent, and poly(vinyl pyrrolidone) (PVP, 10 kDa) used as porogen, were purchased from Aldrich (Lyon, France). The CNTs were produced in our laboratories using a catalytic fluidized bed CVD process developed by B. Caussat (LGC, Toulouse, France) and P. Serp (LCC, Toulouse, France) (Corrias *et al.*, 2003; Morancais *et al.*, 2007). The MWCNTs were then purified with sulfuric acid in order to remove the catalyst, which consisted of iron supported by alumina particles. After this treatment, all the alumina was dissolved and less than 2% w/w of iron remains, as deduced from TGA analyses coupled with SEM/EDAX observations (Morancais et al., 2007). The MWCNTs synthesized consistently displayed an external diameter of 10–40 nm corresponding to 7–16 walls; the length could range up to 50 μm. Various properties included in Table 1 were also characterized.

Membrane fabrication. Membranes were made using the wet phase inversion process. The polymer solution was prepared by first mixing CNTs with NMP using a Polytron PT 1300 D homogenizer (Fisher Scientific Bioblock, Illkirch, France) at 23,000 rpm for 10 min. Then PVP and polysulfone were successively added and mixed at 70°C over 20 h to obtain a homogeneous solution. For both blend solutions,

Table 1. Characterization of MWCNTs.

Purity	S_{BET}[a]	*Pore volume*	*Pore diameter (BJH adsorption*[b]*)*	*Raman* I_D/I_G[c]	*Real density*	*Electrical resistivity*	*TPD*[d]
98%	206 m^2/g	0.8–0.89 cm^3/g	6–20 nm	0.6	1.9 g/cm^3	10^{-4} Ohm.cm	total $O_2 = 7$ μmol/g

[a]Brunauer-Emmett-Teller specific surface area; [b]Barret-Joyner-Halenda method; [c]Ratio of the intensity of the G and D bands; [d]Temperature-programmed desorption.

20% w/w of PSF and 15% w/w of PVP were used. The amount of NMP and CNT added was adjusted as a function of the desired composition: 65% w/w of NMP for the pure polymer membrane, and 63.6 and 1.4% w/w of NMP and CNTs, respectively, for the nanocomposite.

The polymer solutions were cast on a glass plate at room temperature (20°C). Three minutes after the casting, the glass plate with polymer solution film was immersed in a water bath at room temperature (20°C), tap water being used as a nonsolvent of the polymer. No CNTs were visually observed in the coagulation bath indicating that CNTs were incorporated into the membrane. The CNT content in the final produced membrane was calculated to be 4% w/w, as the ratio of CNTs to all polymers (PVP and PSF), assuming that all of the solvent was released to the water.

Characterization of the membrane

Morphology. The cross-section of the membranes was observed by scanning electron microscopy (SEM), using a FEI Quanta 400 ESEM FEG (Hillsboro, OR) in a high vacuum mode at 20 kV. SEM was used to detect possible changes in the structure of the membranes cast with nanotubes compared with those cast without CNTs. The analysis also consisted of checking the position and distribution of the nanotubes throughout the material. Cross-sections were obtained by freeze-fracturing the membranes in liquid nitrogen. The samples were sputter-coated with gold for 20 s at 100 mA (Sputter Coater CRC-150, Torr International Inc., New Windsor, NY) prior to the SEM imaging.

Optical interferometry measurements were carried out using a MicroXam vertical scanning interferometer (ADE-phase Shift Technology, Tucson, AZ). Vertical scanning interferometry (VSI) was used to characterize membrane surface morphology and structure. It was possible to obtain large scan sizes of up to a square millimeter with a vertical resolution of approximately 2 nm with VSI. The basic principles of the interferometer are described elsewhere (Luttge *et al.*, 1999). The interferograms were digitized with a CCD camera and converted into a topographic map with MAPVUE software. As the roughness depends on the scan size (Koyuncu *et al.*, 2006), the same scan area (809 × 613 μm) has been used to compare the different samples. Measurements were performed on at least five different locations on each sample. The criterion choosen for the roughness is the root mean square roughness:

$$R_q = \sqrt{\sum_{1}^{N} \frac{(z_n - z_0)^2}{(N-1)}}$$

where z_o is the average of the z values within the given area, z_n the current z value, and N is the number of data points within the given area.

Permeability. Permeability of each 47 mm diameter membrane was measured in a Sterlitech (model HP4750) 300-mL dead-end filtration cell (Kent, WA) with ultrapure water. The cell was directly connected to the pressure regulator of the compressed air tank. Each membrane was first compacted at 38 bars until the flow rate was stable (at least 30 min). Then, the flow rate was measured by weighing the permeate as a function of the pressure applied (between 5 and 35 bars). The test was performed in triplicate.

Contact angle measurements. Contact angles were measured to characterize the hydrophobicity of the membranes. However, such analyses remain difficult to interpret due to surface roughness that creates contact angle hysteresis (Morrow and McCaffery, 1978; Drelich *et al.*, 1996). Measurements were performed using sessile drop and captive bubble methods with an EasyDrop Contact Angle Measuring Instrument (Krüss, Matthews, NC). For the sessile drop technique, a 5-μL drop of pure water was placed onto a dry membrane in air, and the contact angle was measured. As the membrane surface is initially dry, the angle measured as such is representative of the advancing contact angle, θ_A, also obtained by expanding the drop. In the captive bubble method, the membrane was inverted and immersed in a glass chamber filled with water. A 5-μL air bubble was released from the tip of a U-shaped needle and floated under the surface of the membrane. The contact angle as measured with this technique is generally close to the receding angle, θ_R, obtained when air is withdrawn from the bubble causing it to contract (Drelich *et al.*, 1996). The values of the contact angles determined by both methods were averaged over 10 different drops. Hereafter, the contact angles obtained by the sessile-drop method will be referred to as the advancing contact angle, and the receding contact angle will signify the contact angle deduced from the captive bubble technique.

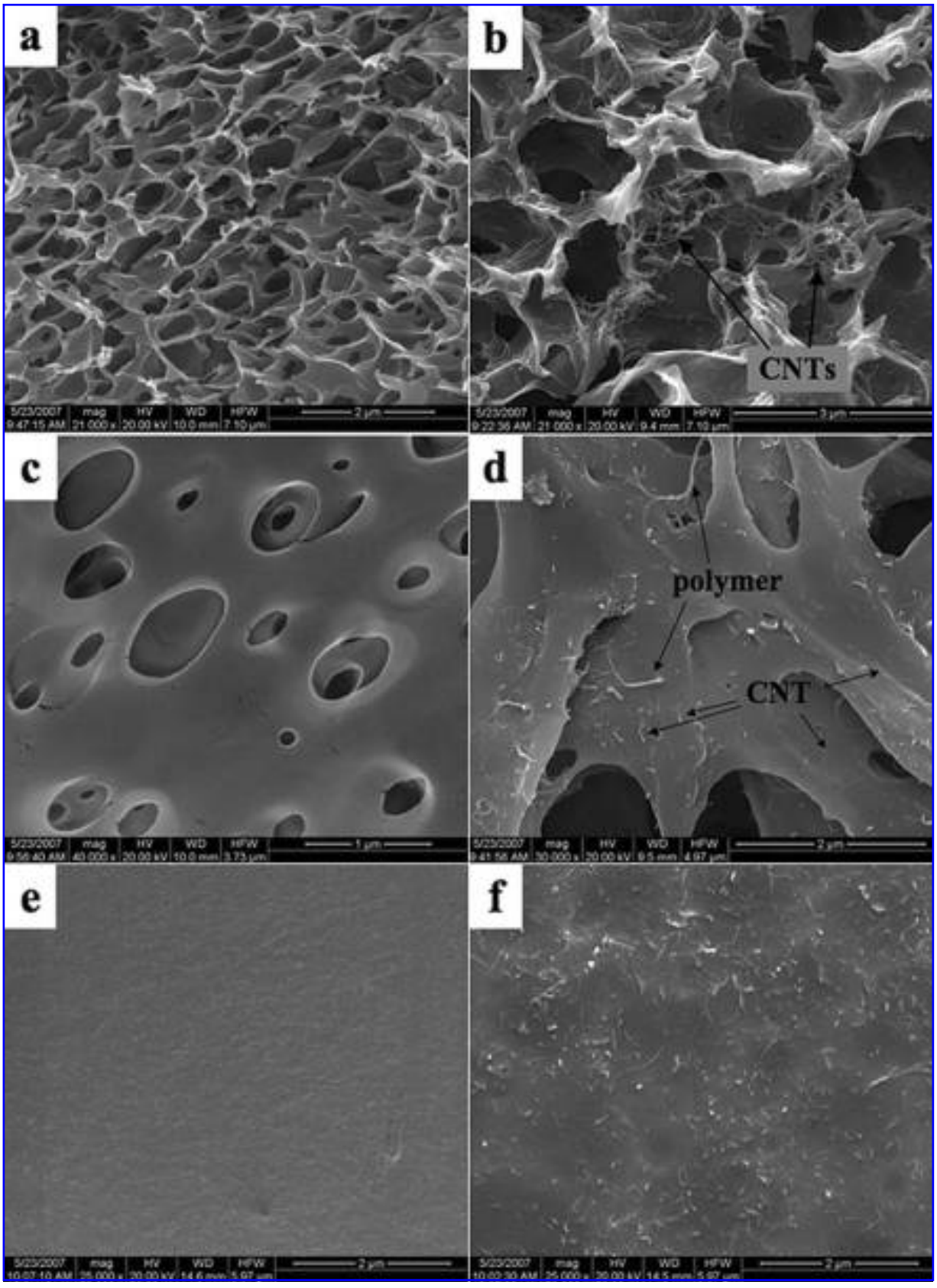

Figure 1. High magnification SEM images of the cross-section and the surface of the membrane without CNTs (left column) and with CNTs (right column). Cross-section of the fine pore structure of the control membrane sublayer (**a**) and the nanocomposite membrane sublayer (**b**); macrovoids internal surface of the control membrane (**c**) and of the membrane containing CNTs (**d**); top view of the membrane surface without CNTs (**e**) and with CNTs (**f**).

Mechanical properties. Tensile properties of membranes were measured on die cut dog bone test coupons (63.5 mm length and 3.3 mm width). The main parameters of interest are tensile strength, elastic modulus, and percentage of elongation. All membrane coupons investigated (at least five specimens per composition) were cut along the same axis. A few more were cut perpendicularly to assess the isotropy of the membrane. The experiments were conducted at room temperature using a tensile testing machine (Instron model 4500, Canton, MA), with an extension rate of 1 mm/min.

Bacteria/nanotubes and bacteria/membranes interactions

The antibacterial activity of CNTs was assessed both in a suspension and as incorporated into membranes against the Gram-negative bacterium *Escherichia coli* K12 (ATCC 10798). To investigate the effect of CNTs on bacterial growth and adhesion on membranes, two complementary techniques were used. The membranes were either placed on agar plates with bacteria deposited by filtration or immerged in a batch culture of stressed cells. Bacteria were maintained either in Luria Bertani (LB) broth or on LB plates at 37°C. Where noted, a defined medium termed minimal Davis medium (MD) was used (Lyon *et al.*, 2005).

E. coli *exposed to CNTs in an agar suspension.* Due to the insolubility of CNTs in water, MD plates were overlaid with 5-mL MD agar (16% w/v agar) containing 4 mg/mL CNT or no CNT as a positive control. Fifty microliters of an overnight culture of *E. coli* K12 in LB were plated to form a bacterial lawn, and the plates were monitored for zones of inhibition around the CNT clusters. The experiment was performed in triplicate.

Growth of E. coli *on agar-supported membranes.* An overnight culture of *E. coli* K12 in LB was diluted in MD to a working OD_{600} of 0.001 and then serially diluted to obtain a final dilution of 10^{-8} in 3-mL MD media. The 3-mL cell suspensions were filtered onto membranes which had been autoclaved in water, with the skin layer side up, using a positive-pressure filtration cell. The membranes were placed onto LB agar plates and incubated at 37°C overnight. The plates were visually evaluated for growth. The test was performed in triplicate.

Adhesion and growth on membranes in an E. coli *suspension.* Coupons (1 cm^2) cut from the membranes were immersed in a stationary phase culture of *E. coli* K12 in MD for 3 h. The membranes were then rinsed in water prior to differential staining using 5-cyano-2,3-ditolyl tetrazolium chloride (CTC) and 4′,6-diamidino-2-phenylindole (DAPI), as described by Huang *et al.* (1995). DAPI stains the nucleic acids of all the bacteria attached to the membrane, and CTC stains only cells which are actively respiring, or alive. Briefly, the membrane coupons were stained with 0.05% CTC solution for 30 min, the stain was discarded, and the coupons were fixed with 5% formalin. The formalin was removed, the coupons were rinsed, and they were stained with 1 μg/mL DAPI for 5 min. The coupons were removed from the staining solution, rinsed with water, and then mounted on a glass slide with a coverslip secured with tape to keep it immobile. The coupons were viewed immediately using an Axioplan 2 imaging fluorescent microscope (Carl Zeiss

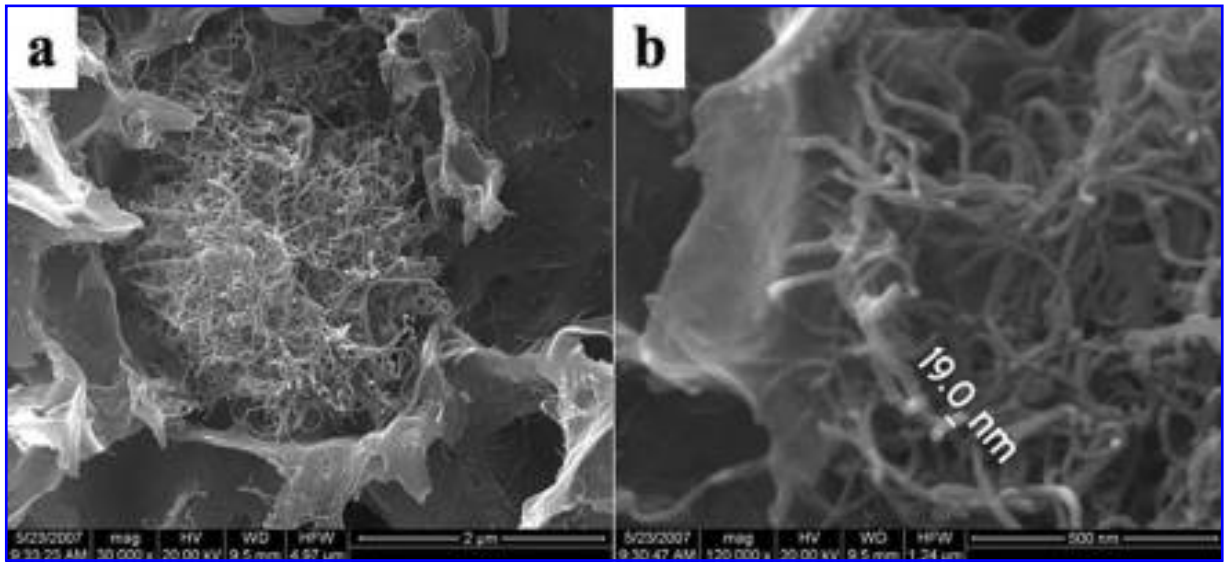

Figure 2. SEM pictures of membranes cross-sections containing nanotubes; (**a**) large aggregate of CNTs nested in a cellular pore; (**b**) higher magnification of CNTs aggregate.

MicroImaging, Inc., Thornwood, NY). To ensure the stains were functioning efficiently, bacteria killed with hydrogen peroxide were stained and examined. Cells that were only stained with DAPI were considered dead, while those stained with both DAPI and CTC were considered alive. The number of live and dead cells were counted and compared for eight samples of each membrane type.

Statistical analysis

Where applicable, standard deviations (SD) and numbers of replicate experiments performed (n) are included. A student *t*-test was used to assess whether differences in membrane properties with and without CNTs were significant at the 95% confidence level.

RESULTS AND DISCUSSION

Dispersion of the nanotubes

The distribution of CNTs was observed in the fractured specimen using SEM. Figure 1 shows high magnification images of the cross-section and surface of membranes containing nanotubes and compares these images to the pure polymeric control membrane. Figure 2 shows additional images of CNTs. Elemental analysis was performed with EDAX, but did not distinguish the CNTs from the polymeric matrix. However, the comparison between the control membrane and the membrane with CNTs in Fig. 1 confirmed that the tubular shapes observed were actually CNTs instead of polymeric fibers. Figure 2b also clearly captured the nanotubes, at a magnification high enough for their diameter to be measured. The diameter measured (19 nm) was in the range of the CNTs produced in our laboratories.

In Figure 1b and 1d, some isolated nanotubes were blended with the matrix and possibly wrapped by a thin layer of polymer. However, there is typically a partial deaggregation of initially tangled bundles (mean diameter of the CNTs agglomerates = 35 μm, after fabrication), leading to aggregates with widely varying diameters of 1 to 10 μm (Figs. 1b and 2b). These aggregates were partly blended with the polymer (Fig. 1b) and sometimes nested in the cellular pores with very little contact with the matrix (Fig. 2b).

The distribution of aggregated or nonaggregated nanotubes was even throughout the material, showing that neither the effect of the solvent carrying the CNTs toward the top layer nor gravity have a dominant effect on the movement of CNTs as anticipated, due to the relatively rapid kinetics of coagulation during membrane formation. Many nanotubes were also detected emerging from or embedded in the skin layer (Fig. 1f).

The presence of aggregates in the membrane suggests that the affinity between CNTs and the polysulfone matrix might be relatively weak. However, PVP appears to be a key component in the membrane composition for the dispersion of CNTs and their interfacial bonding with the host polymer. Without PVP, no isolated CNT but only CNT aggregates were found in the membrane (data not shown). This observation is in accordance with the approach reported by O'-Connell *et al.* (2001) who achieved SWCNTs solubilization by wrapping them with macromolecules like PVP. Wrapping CNTs with PVP increases their hydrophilicity, deagglomerates bundles, and should also enhance their affinity for polysulfone.

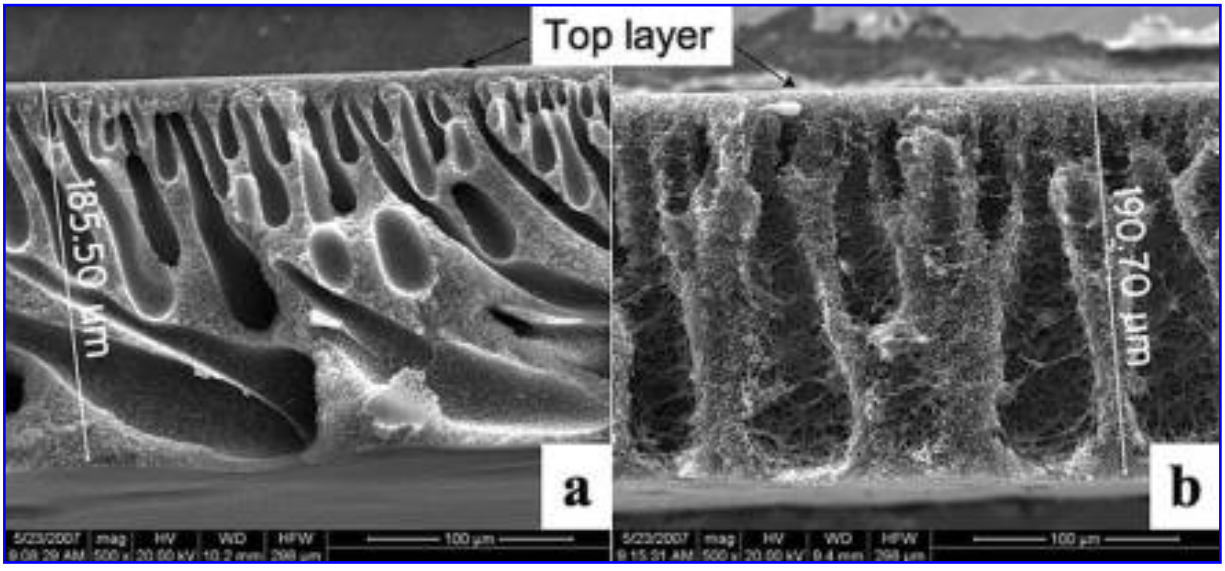

Figure 3. Structure of the membranes without CNT (**a**) and with 4% CNTs (**b**).

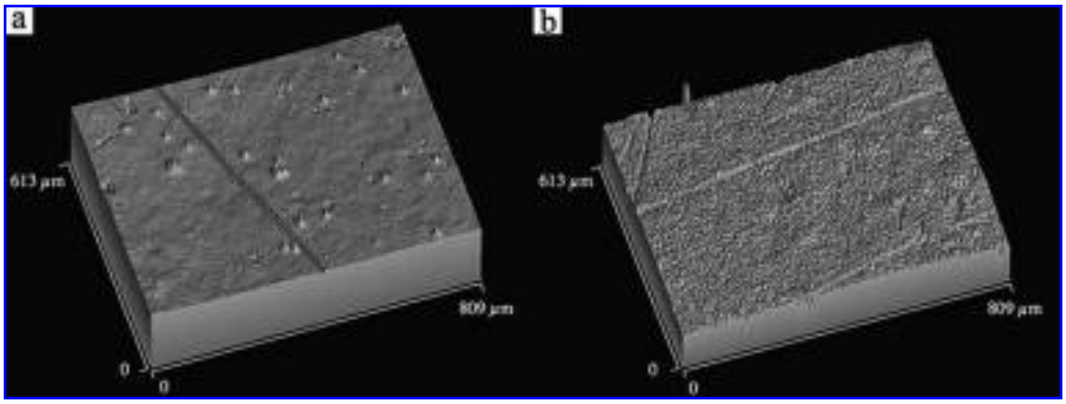

Figure 4. Typical topographic VSI images of the surface of the membranes without CNT (**a**) and with 4% of CNTs (**b**). (Same scale on both images).

Membrane morphology

CNT addition resulted in a uniform dark gray tint of the nanocomposite membrane, whereas regular polysulfone membranes are white. SEM imaging of the two membranes revealed their asymmetric structure. Typically, the control membrane without CNTs, as illustrated by Fig. 3a, exhibited two distinct layers: a very thin skin layer supported by a thick porous layer composed of pores and macrovoids. The macrovoids were adjacent to the top layer and their size increased, moving away from the membrane skin and forming tear-shaped voids. The addition of nanotubes did not significantly change the structure as long as aggregates did not remain too large (Fig. 3b). In tests not shown here, without the addition of PVP which enhances the debundling of CNTs, it was observed that giant agglomerates would completely destabilize the assymetric structure of the membrane or create defects in the skin layer.

Membranes properties

The two membranes were characterized for permeability, surface roughness, and hydrophobicity.

Pure water permeabilities of 24.6 $\pm$ 12.6 and 28.0 $\pm$ 10.7 L/m^2·h·bar were determined respectively for the control and the CNT-amended membranes. These values are statistically undistinguishable at the 95% confidence level. The relatively high standard deviations are due to the heterogeneities in the thickness of the membrane sheets.

VSI was used to scan the surface of the two membranes. Topographic renderings of surface areas of 809 $\times$ 613 μm are shown in Fig. 4a and b. All the membranes exhibited flat surfaces with some scratches resulting from the fabrication process. However, the surface of membranes with nanotubes was rougher with a much more granular or "sandy" appearance than those without nanotubes. Root-mean-square roughness of the surfaces has been calculated from the VSI images and are presented in Fig. 5. When nanotubes were incorporated to the material, the roughness increased by approximately 80%. Judging by the magnitude of the irregularities, the increased membrane roughness is not explained by the emergence of nanotubes through the surface of the top layer. Instead, in Figs. 1f and 5b, the polymeric skin itself shows swellings and depressions. Choi *et al.* (2006) have also observed a similar "nodular" structure. In both cases, it seems that CNTs can work as a destabilizing agent that accelerates the phase separation in the cast solution. This phenomenon overtakes the rheological impact of nanotubes which increases the viscosity of the polymer solution and could thus result in a smoother membrane surface. Finally, the adherence and the proliferation of bacteria on the nanocomposite membrane might be favored in the presence of nanotubes due to the increased roughness of the surface.

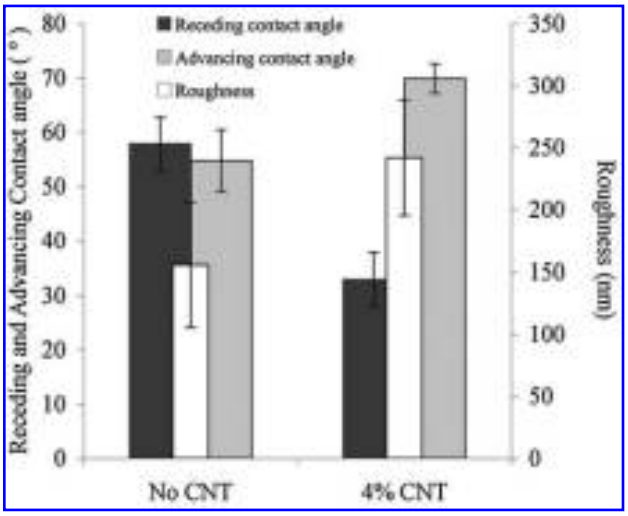

Figure 5. Comparison of the roughness with the receding and advancing contact angles measured for the membrane with and without CNTs.

Table 2. Mechanical properties of the membranes with and without CNTs.

	Control membrane	*Membrane with 4% CNT*
Tensile strength (MPa)	4.2 ± 1.3	4.3 ± 0.1
Elongation at break (%)	25 ± 18	7 ± 1

The contact angles, as determined by sessile drop and captive bubble methods, are presented in Fig. 5 along with the surface roughness acquired by VSI. The hysteresis is the difference between the advancing and receding contact angles. While agreement between the two contact angles was obtained for the smoother control membrane, a clear increase in hysteresis was observed for the membrane containing CNTs. In the nanocomposite membrane, the advancing contact angle increased compared to the pure polymeric membrane while the receding contact angle decreased. The roughness of this membrane partially, if not completely, accounts for this deviation in contact angles. Also, the average between the advancing and the receding contact angles is close to the contact angle obtained for the control membrane. These results suggest that the addition of CNTs to the membrane did not modify its hydrophobicity.

Impact of CNTs on the mechanical properties of the membrane

The percentage of elongation of the samples and the yield tensile strength, equivalent to the ultimate tensile strength, are presented in Table 2 (mean ± standard deviation, $n = 5$). Figure 6 compares the stress–strain behavior of coupons of membranes with or without nanotubes.

With 4% CNT, no effect was observed on the tensile strength. According to the SEM pictures, some entangled bundles were still not deaggregated and barely coated with the polymer. That means that, even if nanotubes are partially dispersed in the membrane, the degree of deaggregation and interfacial bonding is not extended enough to achieve an efficient transfer of their mechanical properties or that the presence of too many aggregates compromises the benefits provided by the deaggregated CNTs.

The composite specimens also showed a drastic decrease in elongation when CNTs are involved. Table 2 shows the elongation-to-failure data with the corresponding standard deviation. The data for the sample without CNT varied over a large range. The nanocomposite material behaved more consistently, but it fractured at a lower level of strain. On average, the elongation to failure decreased by 73% compared to membranes without CNT. The tests performed on samples cut in different directions displayed the same results, suggesting that the membranes are isotropic.

Apparently, the nanocomposite membrane was not reinforced by the ultrastrong CNTs. Reinforced membranes should be characterized by an increase in toughness, that is, an increase in tensile strength while the ductility is at least maintained. In our case, tensile strength was not improved, whereas elongation was reduced. This results in a brittle membrane with a compromised ability to endure high pressures. Our composite material suffered from poor dispersion and/or weak stress transfer, preventing exploitation of the mechanical properties of the CNTs. A better dispersion could potentially be achieved with longer mixing time and sonication of the nanotubes in the solvent. Polymer grafting or wrapping also seems very promising, and materials specialists agree that chemically modified nanotubes show the best results as reinforcing fillers (Coleman *et al.*, 2006). Even if functionalization may decrease the mechanical properties (Garg and Sinnott, 1998), this is compensated by the deaggregation of nanotubes which improves solubility in the solvent, thus the dispersion in the matrix, and the better compatibility with the polymer which increases interfacial bonding.

Coleman *et al.* (2006) offered recommendations that should lead to a fully optimized carbon nanotube–poly-

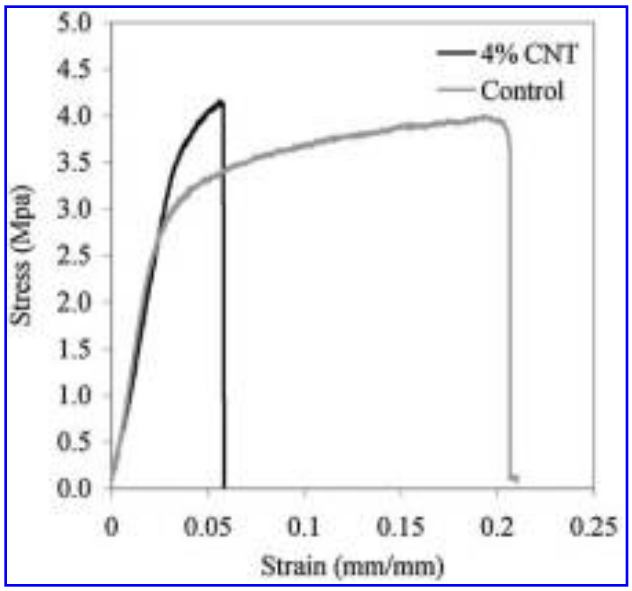

Figure 6. Stress/strain curves for polysulfone membranes with and without CNTs.

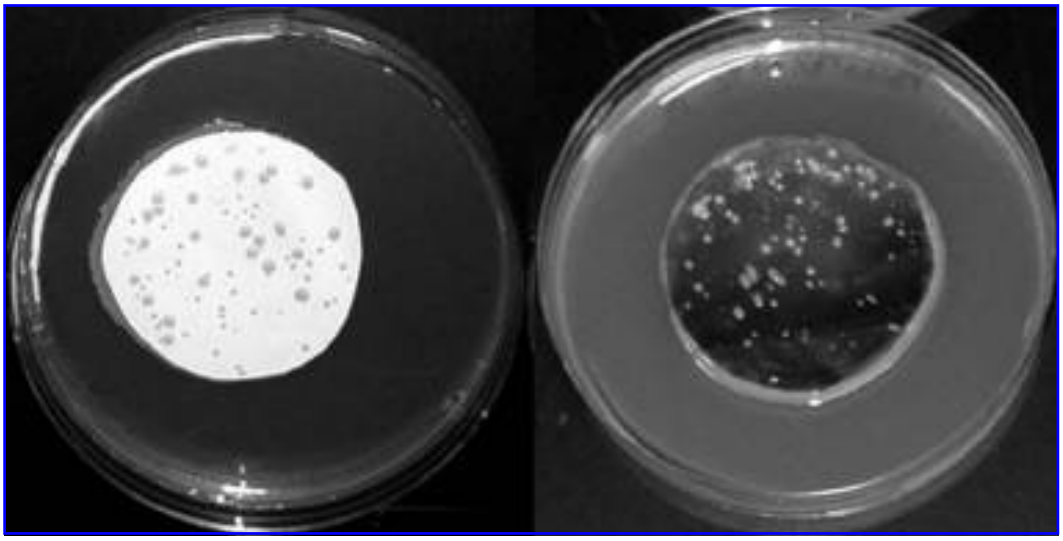

Figure 7. Growth of bacteria on the membrane without CNTs (left) and with 4% of CNTs (right). Each membrane disc has a diameter of 47 mm.

mer composite. Most of the suggestions balance opposing effects. SWCNTs maximize surface area, but can no longer be completely surrounded by matrix beyond a volumetric fraction of 1%. On the other hand, the loading of ideally dispersed MWCNTs with a diameter of ~10 nm could attain a volumic fraction of 25%. Hence, small diameter MWCNTs instead of SWCNTs would optimize both surface area and volume fraction. Also, CNTs should be long enough to maximize strength while not being too long for proper dispersion. One last consideration is the alignment of the CNTs, which may or may not be crucial and beneficial depending on the application. In flat membranes, the orientation of CNTs should preferably be random for an anisotropic reinforcement, whereas in hollow fibers, alignment of CNTs should improve noticeably mechanical properties.

Impact of nanotubes on the bacteria/membrane interactions

Exposure of E. coli *to CNTs in an agar suspension.* To overcome the insolubility of CNTs, they were suspended in agar prior to exposure to *E. coli*. If there were antibacterial activity, a zone of inhibition showing a lack of growth would be expected around the CNT bundles. Despite some iron remaining from the nanotube fabrication by the CVD process, no inhibition of growth was detected. However, this may also be due to insufficient contact of the bacteria with the insoluble CNTs. In addition, a solution of short carboxylated single-wall nanotubes, which have a greater affinity for the aqueous phase, was tested. These carboxylated CNTs also did not exhibit antibacterial activity toward *E. coli* at concentrations as high as 500 mg/L (data not shown).

Growth of E. coli *on agar-supported membranes.* Antibacterial activity of the CNTs in the membrane was qualified as a function of growth of *E. coli* that had been filtered onto the membrane surface. In this experiment, the appearance of colonies on both the control membrane and the membrane with 4% CNT confirmed that their growth had not been inhibited (Fig. 7). The mean colony-forming unit (CFU) counts were not statistically different at the 95% confidence level, with the control having a mean CFU count of 93.5 ± 7.7 and the 4% CNT having a mean CFU count of 125 ± 25.5. This result corroborates the lack of antibacterial activity of CNT in an agar suspension, as discussed above. With this protocol and the high pressures involved

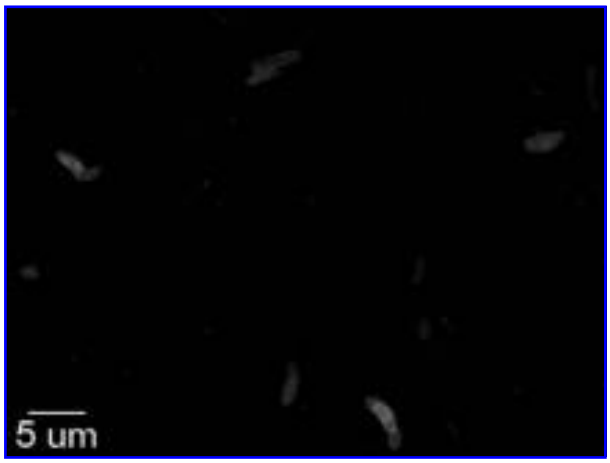

Figure 8. Bacteria adhered to a membrane with 4% of CNTs. CTC die is represented as red, while DAPI is represented with blue. These two colors combined, purple, indicate cells living on the membrane surface.

for the filtration, bacteria were forcibly adhered to the membrane surface; thus, the adherence of the bacteria to the membrane was not an issue. The growth of bacteria indicates that carbon nanotubes do not provide antibacterial properties to the membranes.

Adhesion and growth on membranes in an E. coli *suspension.* To assess the biofouling potential of the membranes, the attachment and viability of *E. coli* to their surface was monitored using fluorescent microscopy. While DAPI stained all bacteria present, CTC stained only the respiring cells. Figure 8 illustrates a typical pattern of live and dead bacteria, stained by one or both the dyes, and grown on the membrane with 4% of CNT. After immersion for 3 h in a culture of nutrient-deprived cells, *E. coli* were able to adhere to the surface of the membranes and remain respiring. To verify the lack of antibacterial activity afforded by the addition of CNT, the number of live versus dead bacteria were counted.

Very few dead cells were detected (8.6 ± 5.8 on the control membrane and 7.8 ± 7.4 on the membrane with CNTs). Over 500 bacteria were counted in total. However, pictures taken did not necessarily display all the bacteria present on the rough membrane but only those in the same focal plane. For this reason, we could not quantify the total number of cells adhered to the membrane. Therefore, we could not verify whether the CNTs would induce a proliferation of the bacteria due to the increased roughness measured with VSI.

In summary, these results indicate that CNTs and membranes with immobilized CNTs did not display antibacterial activity. *A priori*, the dispersion of the CNTs in the polysulfone membranes did not enhance the growth of bacteria. However, this should be confirmed by more extensive tests. We doubt that CNTs are ineffective on account of their concentration in the skin layer (see Fig. 1f) or because the polymer wrapping altered their bioavailability. Instead, the experiments performed with CNTs in suspension suggest that either the CNTs were themselves not antibacterial or their insolubility resulted in a lack of bioavailability and thus no antibacterial activity.

CONCLUSION

The dispersion of carbon nanotubes in a porous structure poses a major hurdle when incorporating such long and entangled nanomaterials into membranes. However, using the common porogen PVP in the membrane was beneficial for the deaggregation of the bundles. Typically, many strands of nanotubes blended with the polymer, but clusters of CNTs also segregated in the pores with only limited contact with the host matrix. Under these conditions, the addition of CNTs did not significantly disturb the morphology of the membrane or the permeability or the hydrophobicity, but an increase of roughness was observed. The partial dispersion of CNTs prevented the host polymer material from taking on the mechanical properties of the CNTs. Finally, due to their lack of toxicity or lack of compatibility with aqueous media and bacteria, CNTs in suspension did not exert antibacterial activity, in contrast with the antibacterial activity reported for other fullerenes (Fortner *et al.*, 2005; Lyon *et al.*, 2005). CNTs dispersed in membranes did not prevent growth nor adherence of cells. Knowing that functionalization will improve the bioavailability of CNTs but will decrease their toxicity (Sayes *et al.*, 2006), CNTs seem to be the wrong candidates for antibacterial fillers to reduce biofouling. Therefore, the main benefits of incorporating CNTs would be the reinforcement of polymeric membranes, which may be better achieved by enhancing dispersion with longer mixing and sonication times and either polymer wrapping or functionalization with groups miscible with the host matrix.

ACKNOWLEDGMENTS

This research was supported by EPA-STAR (91650901-0) and NSF (BES-0508207).

AUTHOR DISCLOSURE STATEMENT

The authors declare that no financial interests exist.

REFERENCES

BARRERA, E.V. (2000). Key methods for developing single-wall nanotube composites. *JOM-J. Min. Metal Mater. Sci.* **52,** A38.

CHOI, J.-H., JEGAL, J., and KIM, W.-K. (2006). Fabrication and characterization of multi-walled carbon nanotubes/polymer blend membranes. *J. Membr. Sci.* **284,** 406.

COLEMAN, J.N., KHAN, U., and GUN'KO, Y.K. (2006). Mechanical reinforcement of polymers using carbon nanotubes. *Adv. Mater.* **18,** 689.

CORRIAS, M., CAUSSAT, B., AYRAL, A., DURAND, J., KIHN, Y., KALCK, P., and SERP, P. (2003). Carbon nanotubes produced by fluidized bed catalytic CVD: first approach of the process. *Chem. Eng. Sci.* **58,** 4475.

DING, L.H., STILWELL, J., ZHANG, T.T., ELBOUDWAREJ, O., JIANG, H.J., SELEGUE, J.P., COOKE, P.A., GRAY, J.W., and CHEN, F.Q.F. (2005). Molecular characterization of the cytotoxic mechanism of multiwall carbon nanotubes and nano-onions on human skin fibroblast. *Nano Lett.* **5,** 2448.

DRELICH, J., MILLER, J.D., and GOOD, R.J. (1995). The effect of drop (bubble) on advancing and receding contact angle for heterogeneous and rough solid surfaces as observed with sessile-drop and captive-bubble techniques. *J.Coloid. Interface Sci.* **179,** 37.

FORTNER, J.D., LYON, D.Y., SAYES, C.M., BOYD, A.M., FALKNER, J.C., HOTZE, E.M., ALEMANY, L.B., TAO, Y.J., GUO, W., AUSMAN, K.D., *et al*. (2005). C60 in water: Nanocrystal formation and microbial response. *Environ. Sci. Technol.* **39,** 4307.

GARG, A., and SINNOTT, S.B. (1998). Effect of chemical functionalization on the mechanical properties of carbon nanotubes. *Chem. Phys. Lett.* **295,** 273.

HUANG, C.T., YU, F.P., MCFETERS, G.A., and STEWART, P.S. (1995). Nonuniform spatial patterns of respiratory activity within biofilms during disinfection. *Appl. Environ. Microbiol.* **61,** 2252.

IIJIMA, S. (1991). Helical microtubules of graphitic carbon. *Nature* **354,** 56.

KEARNS, J.C., and SHAMBAUGH, R.L. (2002). Polypropylene fibers reinforced with carbon nanotubes. *J. Appl. Polym. Sci.* **86,** 2079.

KOYUNCU, I., BRANT, J., LUTTGE, A., and WIESNER, M.R. (2006). A comparison of vertical scanning interferometry (VSI) and atomic force microscopy (AFM) for characterizing membrane surface topography. *J. Membr. Sci.* **278,** 410.

LAM, C.W., JAMES, J.T., MCCLUSKEY, R., AREPALLI, S., and HUNTER, R.L. (2006). A review of carbon nanotube toxicity and assessment of potential occupational and environmental health risks. *Crit. Rev. Toxicol.* **36,** 189.

LUTTGE, A., BOLTON, E.W., and LASAGA, A.C. (1999). An interferometric study of the dissolution kinetics of anorthite: The role of reactive surface area. *Am. J. Sci.* **299,** 652.

LYON, D.Y., FORTNER, J.D., SAYES, C.M., COLVIN, V.L., and HUGHES, J.B. (2005). Bacterial cell association and antimicrobial activity of a C-60 water suspension. *Environ. Toxicol. Chem.* **24,** 2757.

MORANCAIS, A., CAUSSAT, B., KIHN, Y., SERP, P., KALCK, P., PLEE, D., GAILLARD, P., and BERNARD, D. (2007). Large scale production of multi-walled carbon nanotubes by fluidized bed catalytic vapor deposition: A parametric study. *Carbon* **45**(3), 624.

MORROW, N.R., and McCAFFERY F.G. (1978). Displacement studies in uniformly wetted pourous media. In G.F. Padday, Eds. *Wetting, Spreading and Andhesion*, New York: Academic Press, p. 289

NARAYAN, R.J., BERRY, C.J., and BRIGMON, R.L. (2005). Structural and biological properties of carbon nanotube composite films. *Mater. Sci. Eng. B* **123,** 123.

O'CONNELL, M.J., BOUL, P., ERICSON, L.M., HUFFMAN, C., WANG, Y.H., HAROZ, E., KUPER, C., TOUR, J., AUSMAN, K.D., and SMALLEY, R.E. (2001). Reversible water-solubilization of single-walled carbon nanotubes by polymer wrapping. *Chem. Phys. Lett.* **342,** 265.

ROJAS-CHAPANA, J., TROSZCZYNSKA, J., FIRKOWSKA, I., MORSCZECK, C., and GIERSIG, M. (2005). Multi-walled carbon nanotubes for plasmid delivery into *Escherichia coli* cells. *Lab Chip* **5,** 536.

SAFADI, B., ANDREWS, R., and GRULKE, E.A. (2002). Multiwalled carbon nanotube polymer composites: Synthesis and characterization of thin films. *J. Appl. Polym. Sci.* **84,** 2660.

SAYES, C.M., LIANG, F., HUDSON, J.L., MENDEZ, J., GUO, W.H., BEACH, J.M., MOORE, V.C., DOYLE, C.D., WEST, J.L., BILLUPS, W.E., AUSMAN, K.D., *et al.* (2006). Functionalization density dependence of single-walled carbon nanotubes cytotoxicity in vitro. *Toxicol. Lett.* **161,** 135.